Interactions of Fluoroquinolone Antibacterial Agents with Aqueous Chlorine: Reaction Kinetics, Mechanisms, and Transformation Pathways

MICHAEL C. DODD,[†] AMISHA D. SHAH,[‡] URS VON GUNTEN,[†] AND CHING-HUA HUANG*,[‡]

Swiss Federal Institute of Aquatic Science and Technology (EAWAG), Duebendorf, Switzerland CH-8600, and School of Civil and Environmental Engineering, Georgia Institute of Technology, Atlanta, Georgia 30332

Kinetics, products, and mechanistic aspects of reactions between free available chlorine (HOCl/OCl⁻), ciprofloxacin (CF), and enrofloxacin (EF) were extensively investigated to elucidate the behavior of fluoroquinolone antibacterial agents during water chlorination processes. Although the molecular structures of these two substrates differ only with respect to degree of N(4) amine alkylation, CF and EF exhibit markedly different HOCl reaction kinetics and transformation pathways. HOCl reacts very rapidly at CF's secondary N(4) amine, forming a chloramine intermediate that spontaneously decays in aqueous solution by concerted piperazine fragmentation. In contrast, HOCl reacts relatively slowly at EF's tertiary N(4) amine, apparently forming a highly reactive chlorammonium intermediate (R_3N-$(4)Cl^+$) that can catalytically halogenate EF or other substrates present in solution. Flumequine, a fluoroquinolone that lacks the characteristic piperazine ring, exhibits no apparent reactivity toward HOCl but appears to undergo facile halodecarboxylation in the presence of $R_3N(4)$-Cl^+ species derived from EF. Measured reaction kinetics were validated in real water matrixes by modeling CF and EF losses in the presence of free chlorine residuals. Combined chlorine (CC) kinetics were determined under selected conditions to evaluate the potential significance of reactions with chloramines. CF's rapid kinetics in direct reactions with HOCl, and relatively high reactivity toward CC, indicate that secondary amine-containing fluoroquinolones should be readily transformed during chlorination of real waters, whether applied chlorine doses are present as free or combined residuals. However, EF's slower HOCl reaction kinetics, recalcitrance toward CC, and participation in the catalytic halogenation cycle described herein suggest that tertiary amine-containing fluoroquinolones will be comparatively stable during most full-scale water chlorination processes.

* Corresponding author phone: (404)894-7694; fax: (404)894-8266; e-mail: ching-hua.huang@ce.gatech.edu.
† Swiss Federal Institute of Aquatic Science and Technology (EAWAG).
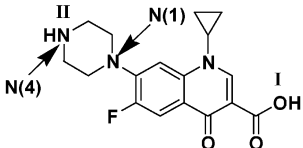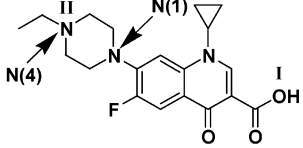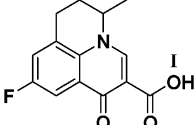‡ Georgia Institute of Technology.

Introduction

Fluoroquinolones currently represent one of the most important classes of antibacterial agents worldwide, on the basis of annual global sales and therapeutic versatility (*1*). They are a family of synthetic, broad-spectrum antibacterial compounds, used in a multitude of human and veterinary applications (*2*). Ciprofloxacin (CF, Table 1) — one of the most frequently prescribed human-use fluoroquinolones in North America and Europe—accounted for nearly $1.3 billion in global sales on its own in 1997 (*1*). Because of the incomplete metabolism of these compounds within the human body (*3–5*), a large fraction of the total clinically prescribed fluoroquinolone load is discharged into municipal wastewater systems (*6*), which represent a principal avenue for entry of such human-use antibacterial agents into the natural aquatic environment (*7, 8*). Various fluoroquinolones have been repeatedly detected at concentrations ranging from ~1–125 µg/L in untreated hospital sewage, ~70–500 ng/L in secondary wastewater effluents, and ~10–120 ng/L in surface waters (*6, 8–13*).

The concentration ranges in the first two cases are particularly notable, because fluoroquinolone MICs (minimal inhibitory concentrations or the lowest concentrations at which bacterial growth is measurably inhibited) extend down to roughly 2–5 µg/L for various bacterial species, including *E. coli* and common *Aeromonas* and *Pseudomonas* strains (*14*). Continuous exposure of bacterial communities to growth-inhibitory concentrations of antibacterial agents can promote induction or dissemination of resistant bacterial phenotypes (*1, 15, 16*). Induction of fluoroquinolone resistance can also bring about cross-resistance to various other classes of antibacterial agents (*17*). Furthermore, numerous resistance phenotypes (including those for fluoroquinolone resistance) are stable over many bacterial generations even in the absence of selective pressure from the antibacterial compounds themselves (*18–21*). Possible induction of fluoroquinolone-resistance in bacteria residing within affected aquatic systems could therefore be of significance to human health, even if chromosomal mutations leading to resistance occur in isolated environments such as hospital sewage or municipal wastewater, which are spatially and temporally remote from points of extensive human contact. The behavior of fluoroquinolones during relevant water treatment processes clearly plays a significant role in this regard.

Generally, significant fractions of fluoroquinolones appear to be concentrated into biosolids during activated sludge treatment, though approximately 10% of influent fluoroquinolone loads can remain in wastewater effluent even *after* tertiary treatment via coagulation/flocculation/filtration (*8*). Disinfection processes (e.g., chlorination, ozonation, and UV irradiation) appear to result in substantial additional fluoroquinolone transformation prior to final discharge of municipal wastewater effluent into receiving streams (*10, 22*). Considering the prevalence of chlorine in municipal wastewater and drinking water disinfection processes, reactions with aqueous chlorine species likely play a particularly important role in the environmental fate of fluoroquinolones.

The current investigation was undertaken to elucidate the kinetics, products, and mechanistic aspects of reactions between free available chlorine (FAC) and the model fluoroquinolones ciprofloxacin (CF) and enrofloxacin (EF) (Table 1). CF was selected for the reasons discussed above. EF, which was popular for disease prevention and control in the U.S. poultry production industry until recently (*23*), was chosen as a model substrate primarily to facilitate comparison of

TABLE 1. Model Substrates and Chemical Properties

Compound	Structure[a]	Mol. Weight	pK$_a$
Ciprofloxacin (CF)		331.35	pK$_{a1}$ = 6.2, pK$_{a2}$ = 8.8 (68)
Enrofloxacin (EF)		359.39	pK$_{a1}$ = 6.1, pK$_{a2}$ = 7.7 (69)
Flumequine (FLU)		261.25	pK$_{a1}$ = 6.5 (70)

[a] Site(s) of ionization labeled according to number of the corresponding pK$_a$ (e.g., site corresponding to pK$_{a1}$ of CF is labeled "I").

$$K_{a1} = K_{11} + K_{21}$$
$$1/K_{a2} = 1/K_{12} + 1/K_{22}$$
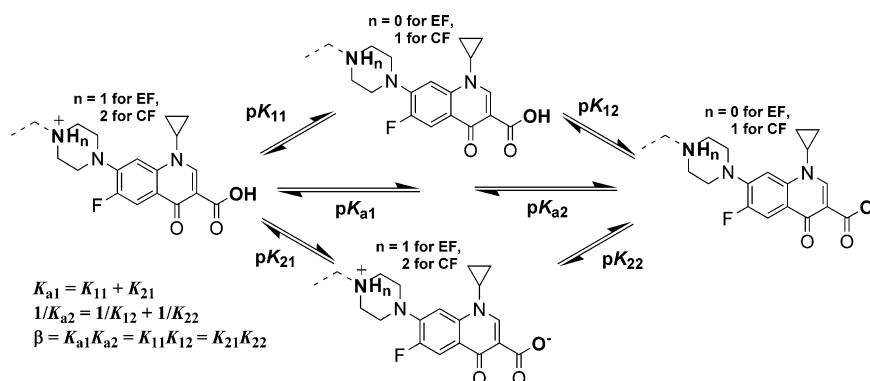$$\beta = K_{a1}K_{a2} = K_{11}K_{12} = K_{21}K_{22}$$

FIGURE 1. Fluoroquinolone speciation patterns.

chemical reactivities and transformation pathways for secondary N(4) amine-containing fluoroquinolones to those of fluoroquinolones containing tertiary N(4) amines. Aside from EF's tertiary N(4)-alkylation, CF and EF are identical (Table 1; refs 68−70). CF and EF (as well as most other fluoroquinolones) are each amphoteric compounds that exhibit the acid−base speciation relationships shown in Figure 1. A second-order reaction kinetics model that accounts for these speciation patterns (24−27) was used to identify each fluoroquinolones' most reactive species and to achieve preliminary identification of the individual functional moieties participating in reactions with FAC. Flumequine (FLU − Table 1)—a first-generation fluoroquinolone that lacks the piperazine ring present in CF and EF—was selected as a model for the fluoroquinolones' aromatic core, to verify the reactive moieties identified by kinetic modeling. LC/MS was utilized in conjunction with supplementary analytical techniques to identify reaction products resulting from reactions of FAC with CF and EF. Confirmation of reactive sites—combined with product identification and evaluation of product evolution and distributions—permitted postulation of the predominant pathways by which each model fluoroquinolone is transformed during reactions with FAC. Additional experiments were conducted to validate measured FAC reaction kinetics in samples of real municipal wastewater and drinking water and to determine the potential significance of reactions involving combined chlorine (CC).

Materials and Methods

Chemicals. CF hydrochloride, EF, and FLU were obtained from ICN Biomedicals (Irvine, CA). CF and 4,6-dichlororesorcinol were obtained from Fluka (Buchs, Switzerland) and Aldrich (St. Louis, MO), respectively. Commercial chemical standards were of at least 97% purity and were used without further purification. NaOCl was obtained from Fisher Scientific (Pittsburgh, PA) or Riedel de Haën (Seelze, Germany) at ∼7% purity. All other reagents used (e.g., buffers, colorimetric agents, reductants, etc.) were obtained from Fisher Scientific or Fluka and were of at least reagent grade quality. All reagent solutions were prepared using water obtained from Nanopure (Barnstead − Dubuque, IA) or MilliQ Ultrapure Gradient A10 (Millipore − Billerica, MA) water purification systems. CF hydrochloride and EF stocks (0.3−3 mM) were prepared in 10−50% methanol. FLU stocks (0.4−4 mM) were prepared in 50−100% methanol. CF stocks of 5−20 mM (used only for determination of CF/FAC reaction kinetics and stoichiometry) were prepared in 0.05 M NaOH. FAC and preformed CC stocks were prepared according to procedures described elsewhere (27) and standardized by iodometry and DPD-FAS titrimetry, respectively (28). Ten-mM acetate (pH 4−5), phosphate (pH 6−8.5), and borate (pH 9−11) buffers were used to maintain constant pH during experiments

TABLE 2. Wastewater (WW) and Drinking Water (DW) Sample Characteristics

water quality data	pH	alkalinity (mg/L as CaCO₃)	NH₃ (mg NH₃—N/L)	DOC (mg/L as C)
Atlanta WW	7.3	120	<0.12[a]	14.0
Atlanta DW	6.6	13	<0.12[a]	1.3
Kloten WW	8.3	143	0.013	5.6
Lake Zurich DW	8.4	126	0.0068	1.6

[a] Minimum detectable concentration was ~120 μg/L NH₃—N (~7 × 10⁻⁶ mol/L) (27).

conducted in reagent water systems. Municipal wastewater and drinking water samples were obtained from Atlanta, GA, and Zurich, Switzerland (see Supporting Information Text S1 for descriptions of sample procurement and process train details). Important water quality parameters for these real water samples are provided in Table 2.

Reaction Monitoring by Analysis of Substrate Loss in the Presence of FAC or CC. *Analytical Methods.* A Hewlett-Packard 1050 HPLC system equipped with a Supelco Discovery RP Amide C16 column (3 mm × 250 mm, 5 μm), fluorescence detector, and single-wavelength UV detector was used to monitor residual EF and FLU in FAC experiments. Other CF, EF, and FLU analyses were conducted with the same equipment described previously for the antibacterial agent sulfamethoxazole (27), except that fluorescence detection (FLD) was used to monitor CF, EF ($\lambda_{ex} = 278$ nm, $\lambda_{em} = 445$ nm), and FLU ($\lambda_{ex} = 312$ nm, $\lambda_{em} = 366$ nm) at concentrations lower than 10 μM, while UV detection ($\lambda = 205$ nm) was used for CF, EF, and FLU concentrations above 10 μM. Analyte and product peaks were resolved via gradient elution with varying proportions of 0.04—0.05 M phosphate buffer (pH ~ 2.1) to acetonitrile in all cases. Typical FLD quantification limits were ~10 nM for CF and EF and ~100 nM for FLU. UV detection limits were ~100 nM for CF, EF, and FLU.

CF and EF experiments were conducted in clean water systems (in triplicate) and real water systems (in duplicate) according to the general procedures described previously for sulfamethoxazole (27), except that excess sodium thiosulfate was used to quench residual oxidant in EF/FAC, CF/FAC, and CF/CC experiments. Suitability of the quenching procedure was verified as described in the Supporting Information, Text S2. Methanol concentrations (from substrate stock solutions) were less than 0.05 vol % (i.e., < 12 mM) in all CF and EF reaction kinetics experiments and should thus have had a negligible effect on rate constant measurements (29—31). Data obtained from CF experiments were used only for evaluation of intermediate decay and product evolution and for estimation of CC kinetics. EF/CC samples were analyzed directly by HPLC, without quenching, and reaction times were corrected for the time delay prior to injection of each sample into the instrument. Duplicate FLU experiments were conducted according to the same procedures as CF and EF (with and without quenching of residual FAC) but only in buffered reagent water. Oxidant controls were included in all experiments to verify the stability of CF, EF, and FLU in aqueous solution. Recoveries of CF and EF from real water matrixes were typically 100 ± 5%.

Calculation of Pseudo-First-Order Rate Constants for Reactions of FAC and CC with EF. Pseudo-first-order rate constants (k'_{obs}) were obtained from the slopes of regression lines fitted to plots of ln([EF]) vs time in the presence of 20× excess FAC. Plots of ln([EF]) vs time were linear in all kinetic experiments, with r^2 values ranging from 0.97 to 1.0 but typically greater than 0.99. The relationship between k'_{obs} and [FAC]₀ was tested at pH 8 and found to be linear from 10:1 to 40:1 [FAC]₀:[EF]₀. A plot of log([FAC]₀) vs log(k'_{obs}) at

this pH yielded a line with slope equal to 1.12 (± 95% confidence interval of 0.09), indicating that the reaction of EF with FAC can be modeled as first order with respect to FAC. Plots of ln([EF]) vs time in the presence of 10× excess CC exhibited poor linearity ($r^2 < 0.95$), due to small total losses of EF (<20%) and substantial losses of CC (> 50%) over the 2.2 d duration of EF/CC experiments, and so were only used to obtain approximate $t_{1/2}$ values for EF transformation.

Calculation of Pseudo-First-Order Rate Constants for Observed Losses of CF in the Presence of Excess FAC or CC. The initial reaction of FAC with CF was too rapid to monitor by the batch methods used for EF/FAC reactions. However, these methods were used to determine the pseudo-first-order rate constant (k'_{frag}) for decay of the chloramine intermediate formed by initial reaction of 10× excess FAC with CF, as will be discussed further in "Results and Discussion." k'_{obs} values for the reactions of CF with 10× excess CC at pH 7 and 9 were determined from linear ($r^2 \geq 0.99$) plots of ln([CF]) vs time. However, additional calculations were necessary to obtain estimates of the pseudo-first-order rate constant, $k'_{initial}$ (for initial reaction between CC and CF) from k'_{obs}, as will be discussed later.

Determination of Pseudo-First-Order Rate Constants for Initial Reaction of FAC with CF. Kinetics for the initial reaction between CF and FAC were studied by two methods: (i) monitoring FAC decay in the presence of excess CF (using a continuous-flow, quenched-reaction apparatus) and (ii) application of competition kinetics (with 4,6-dichlororesorcinol as a reference substrate). Details of these methods are included in Supporting Information, Text S3. Pseudo-first-order rate constants, k'_{obs}, were calculated from linear (0.97 > r^2 > 1) plots of ln([FAC]) vs time (monitored by the continuous-flow method) in the presence of 10—20× excess CF. The relationship between k'_{obs} and dose of CF was tested at pH 5 and found to be linear within the range of 10:1 to 25:1 [CF]₀:[FAC]₀. A plot of log([CF]₀) vs log(k'_{obs}) at this pH yielded a line with slope equal to 1.02 (± 95% confidence interval of 0.26), indicating that the reaction of CF with FAC can be modeled as first order with respect to CF.

Investigation of Catalytic Halogenation Reactions involving EF. Solutions of 0.01 M phosphate buffer (pH 7) were dosed with EF, FLU, and FAC in varying proportion, to evaluate the impact of experimental conditions on EF autotransformation and on EF-catalyzed transformation of secondary substrates (using FLU as a model). These kinetic experiments were conducted by fixing concentrations of two reactants and varying the concentration of the third, using the experimental setup described above. FAC was always added after preparation of solutions containing EF and FLU. Residual EF and FLU concentrations were measured by HPLC, according to the methods described above.

Product Identification. *LC/MS Analyses of Reaction Product Mixtures.* CF, EF, or FLU were added to pH 7 phosphate buffers (0.01—0.1 M) to achieve 100 mg/L (~280—380 μM) starting concentrations. FAC was subsequently added to achieve [FAC]₀:[substrate]₀ ratios of 1:2 to 5:1. Product mixtures resulting from reactions of FAC with CF (unquenched), of FAC with EF (unquenched and quenched with Na₂S₂O₃), and of FAC with EF in the presence of FLU (quenched with Na₂S₂O₃) were analyzed using the same mobile phases, equipment, and instrument settings described in a prior investigation of sulfamethoxazole/FAC reactions (27). HPLC fraction collection was used to isolate samples of CF products observed during kinetic experiments for comparison against peaks observed in product identification experiments, according to the procedures reported for the sulfamethoxazole study (27).

Supplemental LC/MS analyses were conducted at lower concentrations as follows. EF was added to 500 mL of 0.01
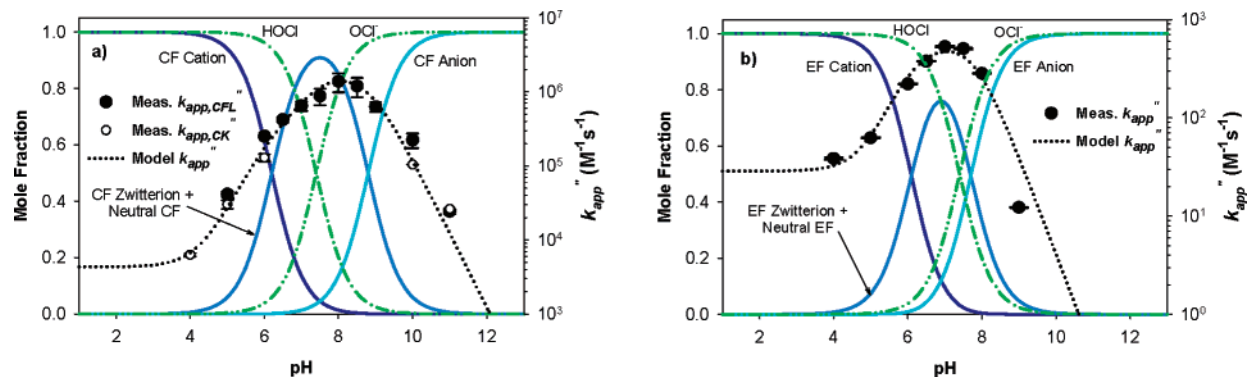
FIGURE 2. pH-dependence of apparent second-order rate constants for fluoroquinolone reactions with FAC: (a) $[CF]_0 = 15-100 \times 10^{-6}$ M, $[FAC]_0 = 1.5-5 \times 10^{-6}$ M, $T = 22 \pm 0.2$ °C, CFL - continuous-flow, CK - competition kinetics and (b) $[EF]_0 = 1.4 \times 10^{-6}$ M, $[FAC]_0 = 2.8 \times 10^{-5}$ M, $T = 25$ °C.

M phosphate buffer at a concentration of 2.8 μM, then dosed with 28 μM of FAC, and allowed to react for 2.5 min before quenching with 500 μM of $Na_2S_2O_3$. This solution was then frozen and freeze-dried via lyophilization until the total volume was reduced to ~20 mL. The remaining solution was evaporated to dryness with N_2 and reconstituted in methanol to a final volume of approximately 1 mL. The 500-fold concentrated sample was then analyzed using an Agilent 1100 HPLC system equipped with a Macherey-Nagel Nucleosil 100-5 C18 HD column (2 mm × 250 mm, 5 μm), column thermostat ($T = 30$ °C), single-wavelength UV detector ($\lambda = 278$ nm), and a Micromass Platform LC single-quadrupole mass spectrometer. Analyte peaks were resolved using gradient elution with varying ratios of 0.2% (v/v) formic acid to pure acetonitrile. MS analyses were conducted using positive mode electrospray ionization (ESI$^+$), over a mass scan range of 50−500 daltons. MS capillary and cone voltages were set to 2.5 and 35 V, respectively. ESI interface temperature was set to 150 °C and drying gas flow was set to 500 L/h.

FAC and CF Reaction Stoichiometry. Stoichiometry of the reaction between FAC and CF was determined by measuring depletion of 20 μM CF (via HPLC, for ratios of $[FAC]_0$:$[CF]_0$ ranging from 1:20 to 1:2) and generation of formaldehyde, at pH 7. The yields of formaldehyde were measured as diacetyldihydrolutidine (*32*) after dosing 10 μM CF with ratios of $[FAC]_0$:$[CF]_0$ varying from 1:10 to 1:2. Each measurement was performed at least 2 h after FAC addition.

Results and Discussion

Kinetics of Reactions with Free Available Chlorine. The initial reactions of CF and EF with FAC are first order with respect to each reactant, and could be described by eq 1,

$$\frac{d[FQ]}{dt} = \frac{d[FAC]}{dt} = -k''_{app}[FAC][FQ] \qquad (1)$$

where [FQ] represents the total concentration (including all acid−base species) of each fluoroquinolone, [FAC] represents the total free chlorine concentration ($[HOCl] + [OCl^-]$), and k''_{app} represents the apparent (speciation-dependent) second-order rate constant for each reaction. k''_{app} was determined under pseudo-first-order conditions by dividing the measured pseudo-first-order rate constant k'_{obs} by the concentration of the reactant (FAC or FQ) in excess. Magnitudes of k''_{app} for CF and EF increased substantially above pH 4— reaching a peak near pH 8 for CF (Figure 2a) and pH 7 for EF (Figure 2b) and then decreased above pH 8. These trends can be attributed to a combination of effects derived from FAC speciation ($HOCl \rightleftharpoons H^+ + OCl^-$) and fluoroquinolone speciation (Figure 1), where successive deprotonation of the

substrates contributes to *increases* in reaction rates and dissociation of HOCl to the weaker oxidant species OCl^- contributes to *decreases* in reaction rates (*24−27*). The pH-dependency of k''_{app} for each fluoroquinolone could be quantitatively modeled by eq 2

$$-k''_{app}[FAC][FQ] = -\sum_{\substack{i=1,2 \\ j=1,2,3}} k_{ij}\alpha_i[FAC]\alpha'_j[FQ] \qquad (2)$$

where α_i and α'_j represent the respective species distribution coefficients for oxidant and substrate, i stands for either of the two oxidant species (HOCl or OCl^-), j for each of the model substrate species (cationic, zwitterion/neutral, or anionic), and k_{ij} for the "species-specific" second-order rate constants corresponding to each combination of i and j. Similar approaches have been successfully utilized to calculate species-specific second-order rate constants in many prior studies addressing the reactions of FAC with compounds possessing acidic or basic functional groups (*24−27, 33*).

Oxidant speciation can be modeled using $pK_a = 7.4$ for HOCl (*34*), and fluoroquinolone speciation can theoretically be modeled according to the macro- *or* microspeciation patterns shown in Figure 1. However, reported values of the microspeciation constants K_{11} and K_{21} (Figure 1) can vary widely for a given fluoroquinolone (*35, 36*), precluding accurate microspeciation modeling. Fluoroquinolone speciation was therefore modeled only according to macrospeciation patterns. As a consequence, the zwitterion and neutral species rate constants for each fluroquinolone were determined together as a single "effective" value, even though relative amine and quinolone moiety reactivities (discussed below) suggest that each neutral species should be substantially more reactive than the corresponding zwitterion. Species-specific and effective second-order rate constants k_{ij} were calculated with associated standard errors according to a nonlinear Marquardt−Levenberg regression analysis (SigmaPlot 2002, SPSS Software). OCl^- reactions did not appear to be significant (Figure 2) and thus were neglected in these calculations, in accord with prior investigations of FAC reaction kinetics (*24−27*). Calculated k_{ij} values and standard errors are summarized for CF and EF in Table 3.

Identification of Reaction Centers. Various experimental evidence indicates that initial reactions of FAC with CF and EF occur at the N(4) amine nitrogen of each substrate's piperazine ring (Table 1). FLU (a fluoroquinolone structure lacking the piperazine ring, as illustrated in Table 1) did not react measurably with excess FAC at pH 4, 7, or 9 during the course of 2-h monitoring periods (data not shown), indicating that the quinolone moiety is recalcitrant to direct reaction with free chlorine during the time-scales typical of this investigation (i.e., 1−2 h). This in turn suggests that FAC

SCHEME 1. Proposed Pathways for Reactions of CF with FAC[a]
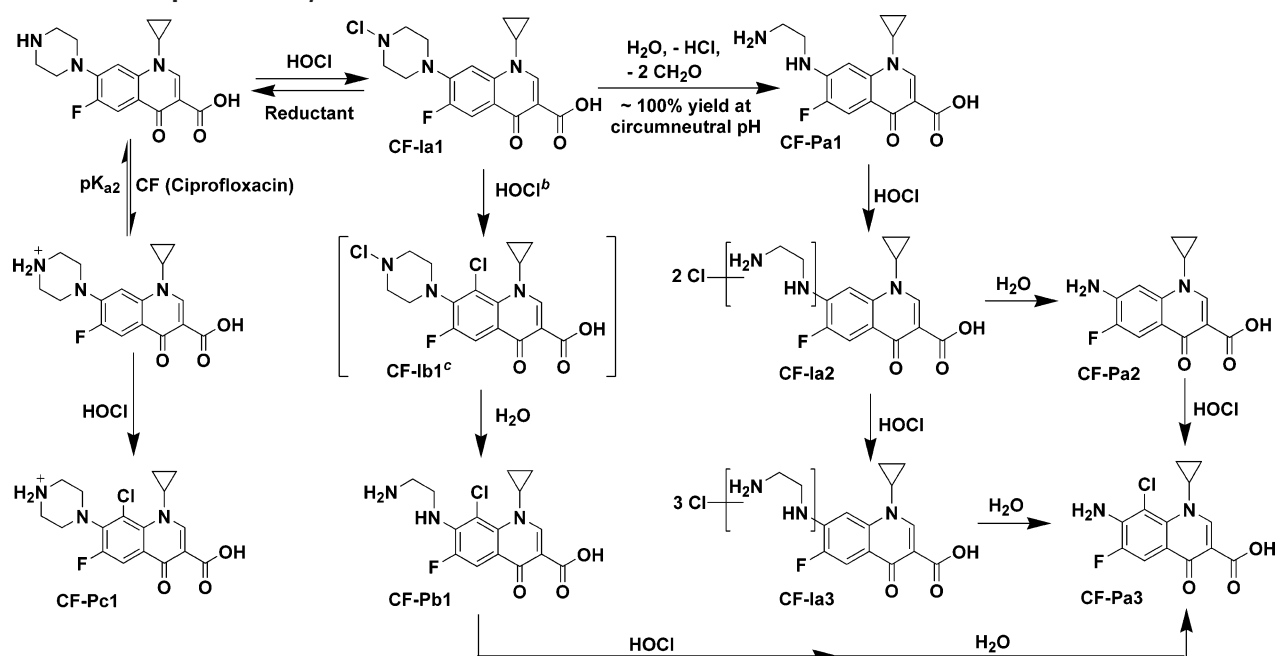
[a] Reaction product structures are postulated on the basis of LC/MS spectra (Supporting Information, Figures S2 and S3) and mechanistic evidence as described herein. [b]Pathway not likely to be important except at very high FAC concentrations, for reasons discussed in the main text. [c]CF-Ib1 was not explicitly observed but is proposed as a probable intermediate on the basis of kinetic constraints, as discussed in the main text.

TABLE 3. Specific Second-Order Rate Constants for Reactions of HOCl with Each Species of CF (at 22 °C) and EF (at 25 °C)

|	species-specific second-order rate constant (M^{-1} s^{-1})		
		effective zwitterion/	
compd	cation (k_{11})	neutral (k_{12})	anion (k_{13})
CF	$4.3 (\pm 6.6) \times 10^3$	$3.8 (\pm 2.4) \times 10^5$	$4.9 (\pm 1.9) \times 10^7$
EF	$2.9 (\pm 0.5) \times 10^1$	$5.4 (\pm 0.2) \times 10^2$	$1.6 (\pm 0.1) \times 10^3$

reacts with CF and EF primarily at their piperazine moieties. Because each piperazine ring's acidic N(1) atom (estimated $pK_a \approx -0.7$ from the SPARC On-line Calculator (37)) should be much less reactive toward electrophilic FAC than the N(4) atom, the latter amine should represent the specific site at which FAC reacts. This is consistent with the substantial increases in observed reactivities of CF and EF toward FAC upon deprotonation of their N(4) atoms (Figure 2, Table 3). Furthermore, the significantly higher reactivity of anionic CF relative to anionic EF is in agreement with typical relative reactivities of neutral secondary and tertiary amines toward FAC (38).

As shown in Table 3, the CF and EF cations also appear to be reactive toward FAC. However, these species' protonated N(4) amines should be inert toward FAC (26, 38, 39), suggesting that FAC reacts slowly with each fluoroquinolone at a secondary site. Although the quinolone moiety represented by FLU is relatively inert toward FAC, the aromatic carbon ortho to CF and EF's piperazine N(1) atom (which is blocked by an alkyl substituent in FLU, as shown in Table 1) should be moderately activated toward reaction with FAC by the presence of the latter compounds' piperazine moieties. One may in turn postulate that the CF and EF cations' apparent reactivity is due to attack at this position. Although each of the other three CF and EF acid–base species should also be susceptible to ortho-halogenation, the relative magnitudes of k_{11} and k_{13} for each substrate (Table 3) illustrate that N(4) chlorination should dominate observed reaction kinetics at circumneutral pH. Products identified from reactions of FAC with CF and EF are consistent with each of

the preceding site-specific reactivity arguments, as will be discussed below.

Product Identification. *Ciprofloxacin.* Postulated structures for products identified from the reactions of FAC with CF are summarized in Scheme 1. Chromatographic and mass spectral data for these products are provided in the Supporting Information (Table S1 and Figures S2 and S3). Addition of FAC to solutions containing CF in molar excess (1:2 $[FAC]_0$:$[CF]_0$, without quenching) led nearly exclusively to generation of the unstable intermediate CF-Ia1 (Scheme 1). Evaluation of this intermediate's LC/MS spectrum (Figure S2a) showed that it contains one Cl atom. A chlorine-free, aqueous sample of CF-Ia1 (isolated by HPLC fraction collection) was reduced to CF upon treatment with $Na_2S_2O_3$, suggesting that CF-Ia1 represents a N-chlorinated variant of CF, because $S_2O_3^{2-}$ and other reduced sulfur compounds are known to reduce chloramines to their parent amine structures (40–44). If such a sample was *not* treated with $Na_2S_2O_3$, CF-Ia1 was observed to decay over the course of 1–2 h to the product CF-Pa1 (Scheme 1, Figure S3b). Measurement of CF loss and formaldehyde yields after addition of various substoichiometric FAC concentrations to pH 7 solutions of excess CF demonstrated that one mole of CF is consumed per mole of FAC added and that two moles of formaldehyde are produced for every mole of CF consumed (data not shown). Addition of molar excesses of FAC to CF solutions resulted in formation of numerous additional reaction products (Supporting Information, Table S1)—the most abundant of which are shown in Scheme 1. Unstable intermediates CF-Ia2 and CF-Ia3 possessed two and three Cl atoms, respectively, as indicated by observed $^{35}Cl/^{37}Cl$ isotopic peak ratios (Figure S2b,c). Treatment with $Na_2S_2O_3$ appeared to reduce each of these intermediates to CF-Pa1, indicating that their Cl atoms are associated with labile N–Cl bonds. An aqueous sample of CF-Ia2 (also isolated via HPLC fraction collection) decayed to CF-Pa2 in the absence of FAC (Figure S3c). Similarly, a sample of CF-Ia3 decayed to CF-Pa3 (Figure S3d) in chlorine-free, aqueous solution. CF-Pb1 appeared to be a monohalogenated variant of CF-Pa1, as suggested by the similar fragmentation patterns evident in

SCHEME 2. Proposed Pathways for Reactions of EF with FAC[a]
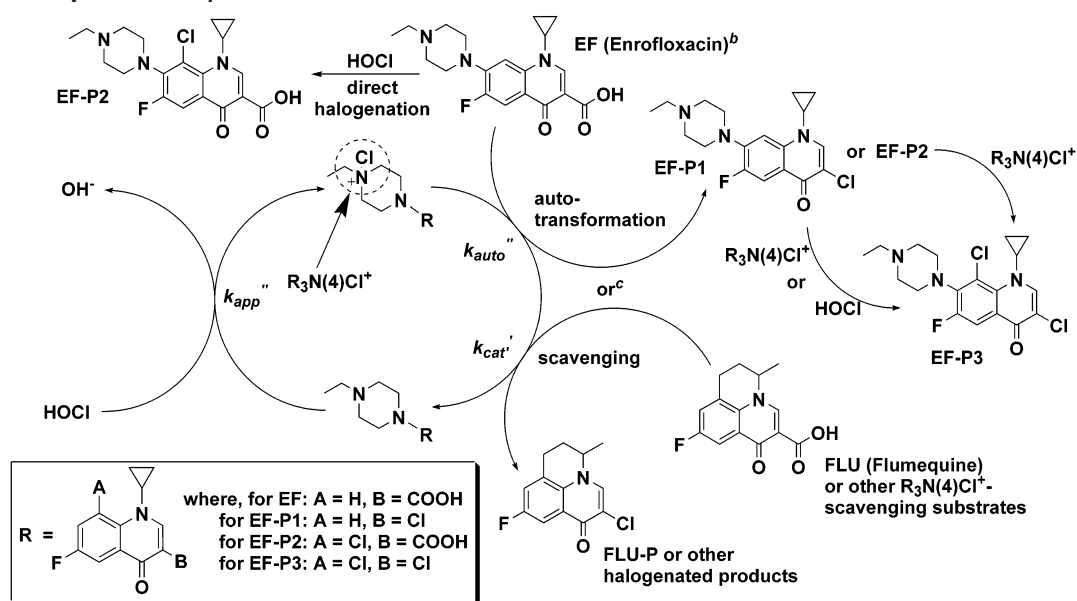
[a] Reaction product structures are postulated on the basis of LC/MS spectra (Supporting Information, Figures S4) and mechanistic considerations as described in the main text. [b] Direct halogenation and autotransformation pathways presumably apply to all four EF acid−base species. [c] Catalytic autotransformation pathways should be suppressed by the presence of $R_3N(4)Cl^+$-scavenging substrates in real water reaction matrixes.

Figure S3b,e. CF-Pc1 was similarly identified as a monohalogenated analogue of CF (Scheme 1, Figures S3a,f). CF-Pa3, CF-Pb1, and CF-Pc1 were all stable in the presence of excess $Na_2S_2O_3$, verifying that their Cl atoms are not associated with reducible N−Cl bonds. Structural assignments of these latter three products' Cl atoms were made on the basis of substitution patterns previously observed for various aromatic amine structures, where halogenation is expected to occur at the position ortho to each molecule's N(1) atom (27, 45, 46).

Enrofloxacin. Postulated structures for products identified from the reactions of FAC with EF are summarized in Scheme 2. Chromatographic and mass spectral data for these products are provided in the Supporting Information (Table S2 and Figure S4). In contrast to CF, no N-chlorinated analogue of EF was explicitly observed, and identifiable EF products all appeared to retain the piperazine moiety (Scheme 2, Figure S4). EF/FAC reactions instead seemed to lead to transformation of EF's quinolone system. EF-P1 was tentatively identified as an EF structure in which the quinolone carboxyl group was displaced by a Cl atom (Figure S4b), on the basis of comparison with EF's LC/MS spectrum (Figure S4a). Decarboxylation (resulting in a mass loss of 45 daltons) and monochlorination (leading to a mass gain of 35 daltons) would yield a net mass loss of 10 daltons relative to the parent EF molecule, in accord with the mass difference between EF and EF-P1. Such a reaction was quite unexpected, because FLU/FAC experiments illustrated that the elementary quinolone structure is essentially nonreactive toward FAC. However, addition of excess FAC to pH 7 solutions containing FLU *and* EF led to substantial consumption of FLU (m/z 262), accompanied by generation of a FLU product with apparent molecular ion of m/z 252 and a Cl-isotope peak at m/z 254 (FLU-P in Figure S5b). The FLU product's mass was also consistent with decarboxylation and halogenation of the parent structure—as indicated by a net mass loss of 10 daltons relative to FLU (Figure S5a). FLU was not measurably degraded during similar experiments conducted with CF in place of EF (data not shown). Taken together, the preceding results indicate that quinolone decarboxylation is catalyzed by EF's tertiary N(4) amine.

Two other products observed by LC/MS were identifiable (EF-P2 and EF-P3 in Scheme 2). EF-P2 appeared to be a

mono-halogenated EF molecule, as evident from the characteristic EF fragmentation patterns in Figure S4c. According to the same reasoning applied to identification of CF-Pc1, the Cl atom in EF-P2 is most likely located ortho to its N(1) atom. Similarly, EF-P3 appeared to be an ortho-halogenated variant of EF-P1 (Figure S4d). The same products were observed in quenched and unquenched reaction solutions dosed with $[FAC]_0 < [EF]_0$ or $[FAC]_0 > [EF]_0$. In addition, each of the EF products shown in Scheme 2 were detected in experiments conducted at high ($[EF]_0 = 280$ μM, $[FAC]_0 = 140-560$ μM) *and* low ($[EF]_0 = 2.8$ μM, $[FAC]_0 = 28$ μM) reactant concentrations.

Proposed Reaction Pathways. *Ciprofloxacin.* CF reacts with HOCl to form the unstable intermediate, CF-Ia1, which subsequently decays to the product CF-Pa1 (Scheme 1) according to eq 3.
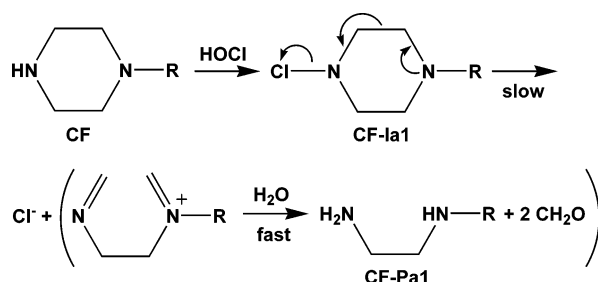
$$CF + HOCl \xrightarrow{k''_{app}} CF - Ia1 \xrightarrow{k_{frag}} CF - Pa1 \qquad (3)$$
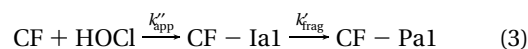
Chloramines possessing an electron-donating, β-heterosubstituent (e.g., N-chloro-α-amino acids and N-chloro-β-alcohols) are generally believed to decay primarily by concerted fragmentation mechanisms (40, 47−49), as depicted below for a generic primary or secondary α-amino acid where R^1, R^2, and R^3 can each represent H or an organic side-chain.
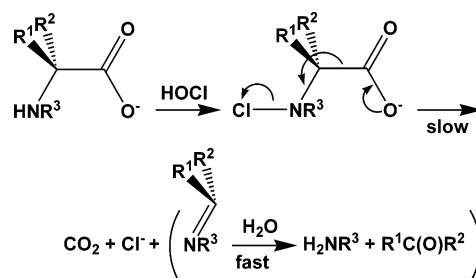
The rate-limiting step of this mechanism is fragmentation/imine formation, which is followed by rapid imine hydrolysis to yield an aldehyde or ketone and the corresponding free amine. Observed stoichiometries of CF consumption and

CH₂O yields during chlorination of CF at neutral pH, coupled with detection of CF-Pa1, are consistent with a similar mechanism (with CF's N(1) amine as the electron-donating heteroatom)where R represents the CF quinolone moiety.

FIGURE 3. CF/FAC transformation product evolution at 25 °C, $[CF]_0 = 1.4 \times 10^{-6}$ M, $[FAC]_0 = 1.5 \times 10^{-5}$ M, and pH = 6.5 (samples quenched with excess Na₂S₂O₃ prior to HPLC analysis). A/A_{max} from FLD signal areas ($\lambda_{ex} = 278$ nm, $\lambda_{em} = 445$ nm).

On the basis of this expression, one can infer that decay of one mole of CF-Ia1 should theoretically yield one mole of CF-Pa1 (Scheme 1), though lack of authentic standards of CF-Pa1 prevented experimental verification of this stoichiometry.

Kinetics of this reaction were evaluated according to the procedures discussed in the "Materials and Methods" section. Because nucleophilic sulfur compounds such as $S_2O_3^{2-}$ and SO_3^{2-} reduce inorganic and organic chloramines to their parent amine structures (40–44), any molecules of CF-Ia1 present in samples of CF/FAC reaction solutions would have been reduced to CF upon addition of thiosulfate. Observed residual CF concentrations in such quenched samples would therefore have been derived in part from any unreacted CF as well as from any CF-Ia1 in the samples prior to quenching. However, the maximum $t_{0.999}$ for CF-Ia1 formation under conditions at which CF reaction monitoring was conducted ($[CF]_0 = 1.4 \times 10^{-6}$ M, $[FAC]_0 = 1.5 \times 10^{-5}$ M) was ~34 s (at pH 4, from the rate constants shown in Figure 2). Therefore, after 60 s of reaction time (corresponding to the earliest time at which samples were taken during monitoring of CF reaction product mixtures), essentially all CF would have reacted to form CF-Ia1, and no free CF would have been present in solution. Consequently, any measured CF would have been derived solely from reduction of CF-Ia1 to its parent amine structure. Thus, the rate constant, k'_{frag}, for decay of CF-Ia1 could be taken to govern the *observed* rate of CF loss in eq 3, according to eq 4.

$$\text{CF-Ia1} \xrightarrow{k'_{obs} = k'_{frag}} \text{CF-Pa1} \qquad (4)$$

k'_{frag} was in turn calculated from linear ($r^2 > 0.99$) plots of $\ln([CF]) = \ln([CF\text{-Ia1}])$ vs time. This rate constant appeared to be independent of FAC dosages between 1.5 and 6 μM at pH 7 (Supporting Information, Figure S6), in agreement with the proposed decay mechanism. However, k'_{frag} was dependent on pH, varying from 2.4 to 7.6 × 10⁻⁴ s⁻¹ between pH 4.6 and 8.6 (Figure S7). The increase in magnitude of k'_{frag} as the pH increases is likely due to an increase of electron density at N(1) (the electron-donating group in piperazine fragmentation) upon deprotonation of the carboxyl group (to which N(1) is conjugated), leading to greater destabilization of the bond bridging the two carbon atoms α and β to N(1).

The presence of numerous additional CF transformation products in samples of reaction solutions containing excess FAC indicates that CF-Pa1 reacts further with FAC. Evolution of these products was monitored as described above for CF-Ia1. However, because the reaction kinetics governing evolution of CF/FAC products beyond CF-Pa1 were not known, it was not possible to distinguish subsequent free amine products from their corresponding chloramines in quenched samples. For example, CF-Pa1 may have been
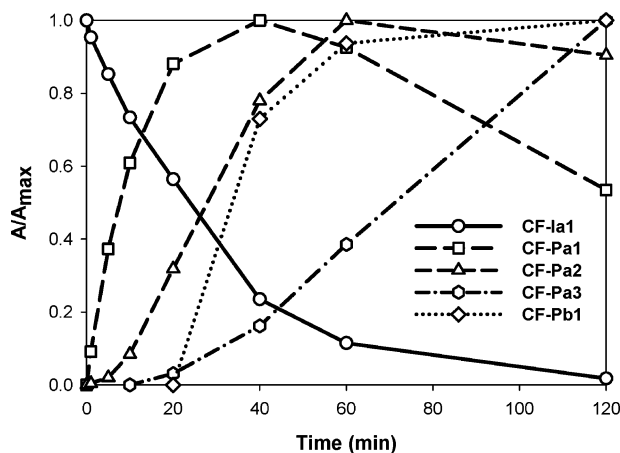
present in CF/FAC reaction solutions at the same time as CF-Ia2 or CF-Ia3. Because the latter two chloramine intermediates are apparently reduced to CF-Pa1 upon treatment with Na₂S₂O₃, any quantity of CF-Pa1 measured by HPLC-FLD in a quenched sample of such reaction solutions could have contained contributions from both unreacted CF-Pa1 and reduced CF-Ia2 or CF-Ia3. Accordingly, the data obtained by this approach were only used to evaluate *qualitative* temporal distributions of *total* amine structure abundance (including unreacted free amines *and* their N-chlorinated structural variants) throughout the evolution of CF/FAC product mixtures, as illustrated in Figure 3.

The data presented in Figure 3 illustrate that decay of CF-Ia1 correlates very well with generation of CF-Pa1. The decrease in CF-Pa1 signal area after roughly 40 min is consistent with further transformation of CF-Pa1 by FAC. N-chlorination of CF-Pa1 presumably leads to production of CF-Ia2 (Scheme 1), which decays to CF-Pa2 in the absence of excess FAC. Decay of CF-Ia2 most likely occurs via concerted fragmentation of its chlorinated ethylenediamine function, in accord with the mechanisms discussed above. The apparent lag in appearance of CF-Pa2 (Figure 3) is consistent with the time required for accumulation of appreciable quantities of CF-Ia2 in solution. Further chlorination of CF-Ia2 presumably leads to CF-Ia3, which decays gradually in solution to yield CF-Pa3. Fragmentation of CF-Ia3's ethylenediamine group should occur in a similar manner as for CF-Ia2. However, the fact that CF-Ia3 decays to CF-Pa3 in the absence of FAC suggests that this process is also accompanied by transfer of a Cl atom from a N–Cl bond to the aromatic quinolone moiety. Similar Cl transfers are known to occur during chlorination of various aromatic amines (27, 45, 46). The extended lag time prior to maximal formation of CF-Pa3 (Figure 3) could be attributable to the time necessary for appreciable quantities of CF-Ia3 to accumulate in solution. However, CF-Pa3 could *also* have formed via direct halogenation of CF-Pa2 by FAC (Scheme 1)—a process that is also consistent with the data shown in Figure 3. It was not possible to determine from available data which of these two possible pathways to CF-Pa3 was dominant.

Formation of CF-Pb1 is believed to proceed through an intermediate, CF-Ib1, generated upon ring halogenation of CF-Ia1 (Scheme 1). Although CF-Ib1 was not explicitly identified, this pathway seems to represent the most plausible route to CF-Pb1 among conceivable alternatives, in consideration of the following kinetic restrictions. Reported rate

constants for various primary amines (*38, 39*) indicate that CF-Pa1's N(4) atom should be orders of magnitude more reactive than the adjacent aromatic ring toward FAC. Consequently, direct halogenation of CF-Pa1 to yield CF-Pb1 would be highly improbable. This implies that halogenation of the quinolone system occurs prior to fragmentation of the piperazine ring. However, direct halogenation of neutral or anionic CF is also unlikely on the basis of known reaction kinetics (Table 3). Therefore, addition of Cl to the aromatic system must occur under conditions for which chlorination of N(4) is unfavorable. The most probable scenario that satisfies this requirement at circumneutral pH is that in which the N(4) atom is already occupied by a Cl atom, as in CF-Ia1. Ortho-halogenation of CF-Ia1's aromatic ring would yield CF-Ib1, which would then decay in the same manner as CF-Ia1, yielding CF-Pb1. Generation of CF-Pb1 should therefore be governed by kinetics associated with CF-Ia1 halogenation. However, the apparent constancy of k'_{frag} of CF-Ia1 at FAC concentrations from 1.5 to 6 μM (Figure S6) indicates that CF-Ia1 halogenation rates are much lower than the rate of CF-Ia1 decay to CF-Pa1 under these conditions. Assuming that halogenation is first order in FAC, this observation implies that generation of CF-Ib1 from CF-Ia1 should be negligible in comparison to CF-Pa1 formation, except at very high FAC concentrations. Further reaction of CF-Pb1 with FAC should yield CF-Pa3 via a reaction pathway similar to that originating from CF-Pa1 (Scheme 1). Therefore, each of the pathways involving CF's neutral or anionic species should ultimately converge to yield CF-Pa3 (Scheme 1). CF-Pa3 is likely to be quite recalcitrant to further reaction with FAC, because it possesses no sites that can be easily chlorinated or oxidized. As a consequence, this product should accumulate over extended reaction times in the presence of excess FAC—in agreement with the data shown in Figure 3.

CF-Pc1 presumably forms via direct halogenation of the CF structure by FAC. This reaction is unlikely to involve the neutral or anionic forms of CF, because the neutral N(4) nitrogens in these species are several orders of magnitude more reactive than the adjacent aromatic rings (see Table 3 and the above discussion in "Identification of Reaction Centers"). Formation of CF-Pc1 is more likely to proceed via reaction of FAC with the CF zwitterion and cation, because these latter species' N(4) amine nitrogens are protonated and essentially nonreactive toward FAC. This pathway should therefore be negligible in comparison to N(4) chlorination at circumneutral pH values, where the deprotonated N(4) amine dominates CF reaction kinetics (Figure 2a). Taken together, the preceding observations indicate that CF should react nearly exclusively via the CF-Pa1 pathway (Scheme 1) under typical water chlorination conditions.

Enrofloxacin. Although the initial reaction of EF with FAC appears to proceed in analogous manner to that of CF (i.e., via chlorination of the N_4 nitrogen), detection of the apparent halodecarboxylation products EF-P1, EF-P3, and FLU-P (Scheme 2) suggests that CF/FAC and EF/FAC reactions subsequently proceed by very different pathways. The mechanism(s) responsible for generation of these products merit(s) particular attention. Electrophilic halodecarboxylation is relatively well documented with respect to bromination and chlorination reactions but only for specific types of substrates (*50–54*). Various mono- and dihydroxybenzoic acid species have been shown to undergo slow halodecarboxylation during treatment with aqueous bromine or chlorine species (*50–53*). Prior investigations also suggest that HOCl can decarboxylate aliphatic β-keto acids (via halogenation of their enol tautomers) (*52, 54*). Each of these reactions can be attributed to the directing effects of activating hydroxyl groups β- to the substrates' carboxyl carbon atoms. The hydroxy-tautomer of the quinolone system (shown here for EF, where R represents the piperazine ring) possesses

such ahydroxy group, but spectral and thermodynamic investigations indicate that the presumably recalcitrant oxo-tautomeric form predominates in aqueous solution (consistent with FLU's stability in the presence of free chlorine) (*55*).
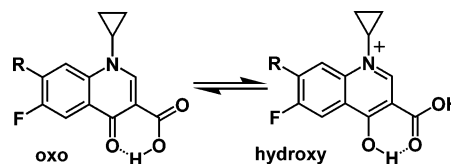
A related explanation for the apparent catalysis of quinolone halodecarboxylation by EF's tertiary N(4) amine could derive in part from the ability of tertiary amines to accelerate enolization of structures analogous to the quinolone β-keto carboxyl group (e.g., oxaloacetic acid) (*56*). However, even if this is the case, the quinolone hydroxy tautomer approximates the structure of salicylic acid, which is itself quite slowly reactive toward HOCl ($k''_{\text{app}} \sim 0.1$ M^{-1} s^{-1} at pH 7.2 (*57*)). This suggests the role of a more reactive halogen species in the observed EF and FLU halodecarboxylations.

Prior investigations have indicated that various tertiary amine compounds (including HEPES and PIPES—which each possess *N*-alkylpiperazine structures) can catalytically accelerate chlorination of molecules such as guanosine, sorbic acid, and salicylic acid. Chlorammonium species (R$_3$NCl$^+$)—which some researchers have suggested may possess chlorinating potential equivalent to or greater than that of molecular chlorine (Cl$_2$) (*58, 59*)—are believed to be responsible for such reactions (*57, 60*). Experimental observations discussed to this point indicate that the R$_3$N(4)Cl$^+$ species generated upon chlorination of EF's tertiary N(4) amine may be similarly responsible for transformation of FLU and for autotransformation of the EF quinolone structure. In this case, catalytic halogenation and decarboxylation of the 4-quinolone system likely proceed according to the following bimolecular mechanism, in which the hydroxy tautomer (I) of a 4-quinolone structure is catalytically halogenated at the 3-position by a mole of R$_3$N(4)Cl$^+$, leading to formation of an unstable intermediate (II) (*51–53*). In analogy to the intermediate formed during bromination of 3,5-dibromo-2-hydroxybenzoic acid (*51*), II should fragment upon deprotonation of its carboxyl group, yielding CO$_2$ and (depending on the parent quinolone) the 3-chlorinated quinolone structures EF-P1, EF-P3, or FLU-P (III).
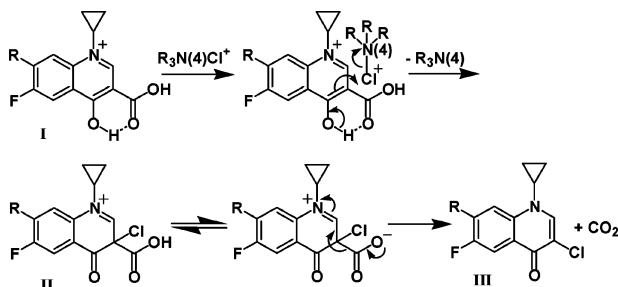
Although one could postulate that quinolone halodecarboxylation might also involve atomic chlorine (possibly formed by homolysis of R$_3$N(4)Cl$^+$), Cl$^\bullet$ should have been effectively scavenged by methanol (typically 2.5–250 mM) present in the reaction system from EF and FLU stocks ($k_{\text{MeOH,Cl}^\bullet} = 1.0\ (\pm\ 0.2) \times 10^9$ M^{-1} s^{-1} (*61*)), permitting one to conclude that the observed halodecarboxylations involve *direct* Cl$^+$-transfer from R$_3$N(4)Cl$^+$. Apparently, R$_3$N(4)Cl$^+$ does not accumulate in EF/FAC reaction solutions to a measurable extent. Measured EF peak areas did not increase upon addition of Na$_2$S$_2$O$_3$ to solutions dosed with EF and a

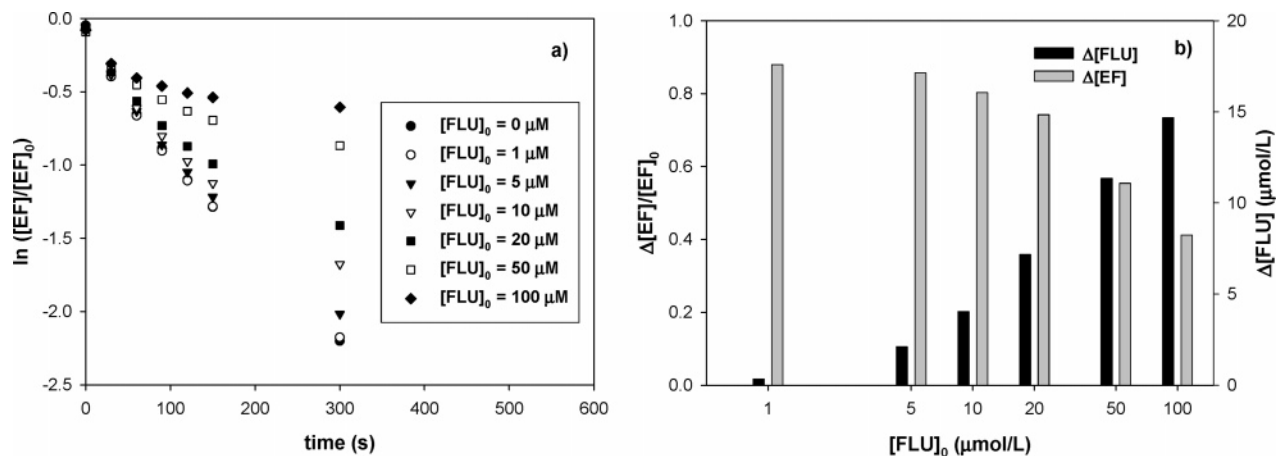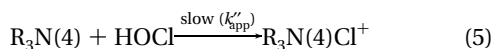**FIGURE 4. Effect of increasing [FLU]$_0$ on EF and FLU transformation at 25 °C, [EF]$_0$ = 1.0 × 10^{-6} M, [FAC]$_0$ = 2.0 × 10^{-5} M, and pH 7: (a) EF decay kinetics in the presence of increasing [FLU]$_0$ and (b) EF and FLU consumption after 300 s of reaction time.**

10-fold excess of FAC, compared to the peak areas observed in corresponding unquenched controls (Supporting Information, Text S2). This observation indicates that R$_3$N(4)Cl$^+$ is depleted significantly faster than it is produced, presumably according to the reactions shown in eqs 5 and 6.

$$R_3N(4) + HOCl \xrightarrow{\text{slow } (k''_{app})} R_3N(4)Cl^+ \qquad (5)$$

$$R_3N(4)Cl^+ + EF \xrightarrow{\text{fast } (k''_{auto})}$$
$$R_3N(4) + EF \text{ halogenation product(s)} \quad (6)$$

Assuming that transformation of the EF structure is due predominantly to reactions with R$_3$N(4)Cl$^+$, transformation rates of EF in EF/FAC reaction systems should be limited by the steady-state concentration [R$_3$N(4)Cl$^+$]$_{ss}$. Therefore, according to eq 6, the decay of EF in FAC reactions can be treated as pseudo-first-order as long as the available concentration of R$_3$N(4)Cl$^+$ remains relatively constant, in turn requiring that [FAC] and [R$_3$N(4)] remain relatively constant, per eq 5. Effectively constant [FAC] was essentially maintained in experiments conducted at [FAC]$_0$ ≫ [EF]$_0$. Considering that the products identified from reactions of FAC with EF (i.e., EF-P1, EF-P2, and EF-P3 in Scheme 2) presumably also yield R$_3$N(4)Cl$^+$ upon N(4) chlorination, it is clear that [R$_3$N-(4)] should have remained essentially constant, as well. The validity of these hypotheses was evaluated by utilizing FLU to selectively scavenge R$_3$N(4)Cl$^+$ from systems containing EF and FAC, according to eq 7.

$$R_3N(4)Cl^+ + FLU \xrightarrow{\text{fast } (k''_{cat})} R_3N(4) + FLU - P \qquad (7)$$
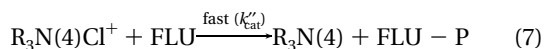
As shown in Figure 4a, increases in solution concentration of FLU resulted in significant deviation of EF decay rates from pseudo-first-order kinetics in the presence of excess [FAC]$_0$. This effect was apparently due to increasing consumption of active chlorine upon addition of higher [FLU]$_0$ to reaction solutions (Figure 4b); that is, FAC was gradually depleted by catalytic transfer of Cl$^+$ from HOCl to FLU via R$_3$N(4)Cl$^+$ (eqs 5 and 6), leading to a continuous decrease in steady-state concentration of R$_3$N(4)Cl$^+$ over the duration of each experiment. These results show that a reaction system's R$_3$N(4)Cl$^+$-scavenging potential significantly influences observed rates of EF transformation, in support of the hypothesis that EF transformation is governed by [R$_3$N(4)Cl$^+$]$_{ss}$.

EF-P1 is apparently formed solely via catalytic autotransformation reaction of EF by R$_3$N(4)Cl$^+$ (Scheme 2). EF-P2 could be formed either via ortho-halogenation of EF by HOCl (consistent with the discussion in "Identification of Reaction

Centers") or ortho-halogenation of EF by R$_3$N(4)Cl$^+$. Similarly, EF-P3 could arise from catalytic halogenation of EF-P1 or EF-P2 or by HOCl halogenation of EF-P1 (Scheme 2). However, the data shown in Figure 4, taken together with the low concentrations at which fluoroquinolones are typically present in real water systems, suggest that catalytic autotransformation reactions would likely be significantly quenched by R$_3$N(4)Cl$^+$-scavenging organic matter in real water matrixes, presumably lowering EF transformation rates and suppressing formation of halodecarboxylation products.

Application of Measured Reaction Kinetics to Real Water Matrixes. *Ciprofloxacin.* Kinetics for initial reaction of FAC with CF could not be monitored directly in real water experiments. However, the CF-Ia1 generated from this reaction decayed in the real water samples at rates very close to those expected on the basis of rate constants determined in reagent water systems (Figure 5a), illustrating that CF-Ia1 decay kinetics are independent of matrix composition. The data presented in Figure 5a also indicate that residual CF concentrations should be substantially reduced during residence times typical of wastewater (5−30 min) and drinking water clearwells (1−24 h). This conclusion is supported by a field study demonstrating degradation of 100 ng CF/L to below detection limits (i.e., < 20 ng/L) during full-scale chlorination of a secondary municipal wastewater effluent (*10*).

However, one must keep in mind that transformation of CF proceeds through CF-Ia1, which can be reduced to CF upon treatment with strong nucleophiles such as SO$_3$$^{2-}$ or S$_2$O$_3$$^{2-}$. Consequently, parent fluoroquinolones such as CF (secondary-N(4)) could be regenerated from N-chlorinated intermediate structures prior to final discharge of effluent from many U.S. wastewater treatment facilities, which commonly use reduced sulfur compounds to dechlorinate disinfected wastewater. In addition, enough FAC was dosed during real water experiments in the current investigation to ensure the presence of *free* chlorine residuals. In many practical applications (e.g., disinfection of wastewater containing high NH$_3$ loads, or chloramination of drinking water), much of an applied chlorine dose may actually be present as *combined* chlorine (primarily NH$_2$Cl, and to a lesser extent NHCl$_2$), for which reaction kinetics are typically considerably slower than for FAC (*42, 62, 63*). In such cases, kinetics of reactions between CC and CF should be taken into account.

Chloramines are known to react with free amines via direct transfer of Cl$^+$ from chloramine to amine (*62, 64, 65*). Thus, the *initial* reactions of CC with CF should proceed according to the same sequence shown in eq 3 for FAC reactions; that is, via formation and decay of CF-Ia1. However, kinetics of CF-Ia1 formation appeared to be sufficiently slow in reactions
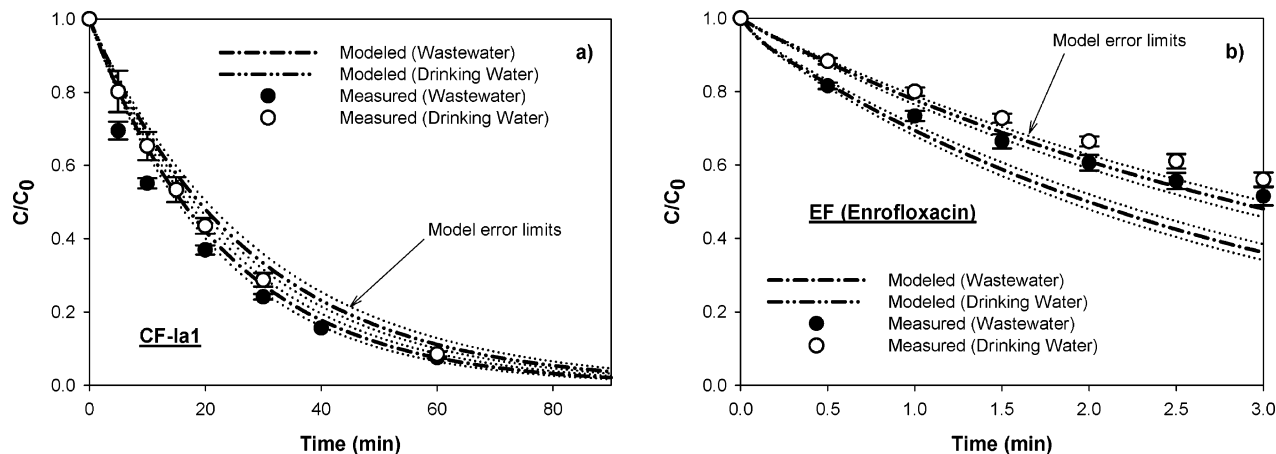
FIGURE 5. Reaction kinetics in real waters at 25 °C: (a) CF-Ia1 — $[CF]_0 = 1.5 \times 10^{-6}$ M, $[FAC]_0 = 1.6 \times 10^{-4}$ M for Atlanta wastewater (pH 7.3) or 2.8×10^{-5} M for Atlanta drinking water (pH 6.6); (b) EF — $[EF]_0 = 1.4 \times 10^{-6}$ M, $[FAC]_0 = 6.3 \times 10^{-5}$ M for Kloten/Opfikon wastewater (pH 8.3) or 3.5×10^{-5} M for Lake Zurich "drinking" water (pH 8.4). Measurement errors are reported as standard deviations of duplicate sample measurements. Error limits for model calculations were determined according to the standard errors determined for CF-Ia1's species-specific, first-order, fragmentation rate constants $k'_{\text{frag,neutral}}$ and $k'_{\text{frag,anion}}$ (Figure S7) and the species-specific second-order rate constants k_{ij} for reaction of EF with FAC (Table 3).

of CF with CC as to be obscured by overlap with the kinetics of CF-Ia1 decay. Thus, the two steps of eq 3 (with CC in place of FAC) were observed as a single step in CC reactions, according to eq 8.

$$CF + CC \xrightarrow{k_{\text{obs}}} CF\text{-Pa1} \qquad (8)$$

Because k'_{frag} is known (Figure S7), the relationship between eqs 3 and 8 could be utilized to model loss of CF according to eqs 9–11, where $\Delta[CF]_{\text{irr}}$ represents total observed, irreversible loss of CF at a given sample time, assuming that one mole of CF decays via CF-Ia1 to yield one mole of CF-Pa1 (according to the earlier discussion of CF-Ia1 fragmentation).

$$\frac{d[CF]}{dt} = k'_{\text{initial}}[CF] \qquad (9)$$

$$\frac{d[CF\text{-Ia1}]}{dt} = k'_{\text{initial}}[CF] - k'_{\text{frag}}[CF\text{-Ia1}] \qquad (10)$$

$$\Delta[CF]_{\text{irr}} = [CF]_0 - ([CF] + [CF\text{-Ia1}]) = [CF]_0 - [CF]_{\text{T}} \qquad (11)$$

Because reaction samples were quenched with $Na_2S_2O_3$, [CF], and [CF-Ia1] were measured together as $[CF]_{\text{T}}$ at each sample time. Substitution of the integrated forms of (9) and (10) into (11) yields eq 12 (66), which was solved for k'_{initial} by nonlinear Marquardt–Levenberg regression (SigmaPlot 2002) of $\Delta[CF]_{\text{irr}}$ measurements vs time.

$$\Delta[CF]_{\text{irr}} = [CF]_0 - [CF]_0 \exp(-k'_{\text{initial}}t) - \frac{k'_{\text{initial}}[CF]_0}{k'_{\text{frag}} - k'_{\text{initial}}} \times [\exp(-k'_{\text{initial}}t) - \exp(-k'_{\text{frag}}t)] \qquad (12)$$

An estimate of 4.4 (± 0.4) $\times 10^{-4}$ s^{-1} ($t_{1/2} \approx 26$ min) was determined for k'_{initial} at pH 7, for 1.4 μM CF dosed with 15 μM CC (which was comprised of ~63% NH_2Cl + ~37% $NHCl_2$, according to DPD-FAS titration), indicating that losses of CF should be relatively extensive even when chlorine doses applied to real waters are present only as CC residuals. Furthermore, the k'_{initial} estimate of 3.6 (± 0.3) $\times 10^{-4}$ s^{-1} ($t_{1/2} \approx 32$ min) obtained at pH 9, for 1.4 μM CF dosed with 15 μM CC (~100% $NHCl_2$), suggests that CF should be readily transformed even in chlorination processes dominated by NH_2Cl. Preliminary LC/MS analyses of CF/CC reaction

solutions indicated that CF was transformed to many of the same products by CC as by FAC (data not shown). However, a detailed study of CC reaction products was beyond the scope of the current investigation.

Enrofloxacin. EF decay in real water samples was modeled according to the same procedures previously used for sulfamethoxazole (27). Rates of EF transformation were moderately slower in environmental matrixes than predicted on the basis of reaction kinetics measured in clean water systems (Figure 5b), likely due in part to suppression of EF autotransformation by $R_3N(4)Cl^+$-scavenging substrates present in the real water matrixes. The likelihood that R_3N-$(4)Cl^+$ will be scavenged by matrix constituents, together with the relatively slow kinetics of direct EF/FAC reactions, indicate that EF and similar fluoroquinolones should generally be less efficiently degraded during chlorination of real waters than secondary-amine containing fluoroquinolones such as CF. In addition, EF and similar tertiary amine-containing fluoroquinolones should be very stable during chlorination of waters containing appreciable quantities of NH_3. Free chlorine applied to such waters should be consumed too rapidly by excess NH_3 (e.g., $t_{1/2} = 0.11$ s for 10 mg/L NH_3–N, at pH 7 (26)) to react to a significant degree with such fluoroquinolones. Furthermore, the approximately 6-day half-life determined for transformation of 1.4 μM EF dosed with 14 μM CC (~75% NH_2Cl + ~25% $NHCl_2$, according to DPD-FAS titration) at pH 7, and 111-day half-life determined under the same conditions at pH 9 (for which $[CC]_0$ was approximately 100% $NHCl_2$) suggest that reactions of CC with such fluoroquinolones will be negligible with respect to the conditions encountered during most water chlorination processes.

Environmental Implications of Fluoroquinolone Structure Transformations. In the absence of biological assay data, toxicological implications of the reactions depicted in Schemes 1 and 2 cannot be determined with certainty. However, fluoroquinolones' ability to inhibit bacterial DNA replication and repair is believed to be linked to their quinolone moieties (67), suggesting that piperazine fragmentation—the predominant pathway by which CF is transformed (Scheme 1)—may not lead to elimination of antibacterial activity. Accordingly, even quinolone structures which lack the piperazine ring (e.g., nalidixic acid) can be active against various types of bacteria (14). Direct halogenation ortho to the piperazine ring (Schemes 1 and 2) is also unlikely to result in elimination of quinolone activity, as

suggested by the considerable antibacterial potency of lomefloxacin (*14*), which is substituted by a fluorine atom in the same position. Although modification of the quinolone moiety via halodecarboxylation (Scheme 2) might interrupt the charge interactions and hydrogen-bonding required for quinolone-DNA binding, this reaction may be relatively unimportant in real waters. On the basis of these observations, one can infer that a majority of the transformation products likely to result from passage of fluoroquinolones through water chlorination processes may retain antibacterial activity.

Acknowledgments

Supporting Information Available

Text, figures, and tables of (1) real water sample procurement, source characteristics, and parameter measurements, (2) quenching of EF/FAC reactions, (3) measurement of CF reaction kinetics, (4) reaction products identified by LC/MS, and (5) the pseudo-first-order rate constant for decay of CF-Ia1. This material is available free of charge via the Internet at http://pubs.acs.org.

Literature Cited

(1) Walsh, C. *Antibiotics: Actions, Origins, Resistance*; ASM Press: Washington, DC, 2003.

(2) National Research Council. *The Use of Drugs in Food Animals*; National Academy Press: Washington, DC, 1999.

(3) Nicolle, L. E. In *Antibiotics in Laboratory Medicine*, 4th ed.; Lorian, V., Ed.; Waverly and Wilkins: Baltimore, MD, 1996; pp 793–812.

(4) Gerding, D. N.; Hughes, C. E.; Bamberger, D. M.; Foxworth, J.; Larson, T. A. In *Antibiotics in Laboratory Medicine*, 4th ed.; Lorian, V., Ed.; Waverly and Wilkins: Baltimore, MD, 1996; pp 835–899.

(5) RxList, The Internet Drug Index (http://www.rxlist.com/top200.htm). NDC Health: Place Published.

(6) Hartmann, A.; Alder, A. C.; Koller, T.; Widmer, R. M. Identification of fluoroquinolone antibiotics as the main source of umuC genotoxicity in native hospital wastewater. *Environ. Toxicol. Chem.* **1998**, *17*, 377–382.

(7) Hirsch, R.; Ternes, T. A.; Haberer, K.; Kratz, K.-L. Occurrence of antibiotics in the environment. *Sci. Tot. Environ.* **1999**, *225*, 109–118.

(8) Golet, E. M.; Xifra, I.; Siegrist, H.; Alder, A. C.; Giger, W. Environmental exposure assessment of fluoroquinolone antibacterial agents from sewage to soil. *Environ. Sci. Technol.* **2003**, *37*, 3243–3249.

(9) Hartmann, A.; Golet, E. M.; Gartiser, S.; Alder, A. C.; Koller, T.; Widmer, R. M. Primary DNA damage but not mutagenicity correlates with ciprofloxacin concentrations in German hospital wastewaters. *Arch. Environ. Contam. Toxicol.* **1999**, *36*, 115–119.

(10) Renew, J. E.; Huang, C.-H. Simultaneous determination of fluoroquinolone, sulfonamide, and trimethoprim antibiotics in wastewater using tandem solid-phase extraction and liquid chromatography-electrospray mass spectrometry. *J. Chromatogr., A* **2004**, *1042*, 113–121.

(11) Miao, X.-S.; Bishay, F.; Chen, M.; Metcalfe, C. D. Occurrence of antimicrobials in the final effluents of wastewater treatment plants in Canada. *Environ. Sci. Technol.* **2004**, *38*, 3542–3550.

(12) Kolpin, D. W.; Furlong, E. T.; Meyer, M. T.; Thurman, E. M.; Zaugg, S. D.; Barber, L. B.; Buxton, H. T. Pharmaceuticals, hormones, and other organic wastewater contaminants in U.S. Streams, 1999−2000: A national reconnaisance. *Environ. Sci. Technol.* **2002**, *36*, 1202−1211.

(13) Golet, E. M.; Alder, A. C.; Giger, W. Environmental exposure and risk assessment of fluoroquinolone antibacterial agents in wastewater and river water of the Glatt Valley watershed, Switzerland. *Environ. Sci. Technol.* **2002**, *36*, 3645−3651.

(14) Wiedemann, B.; Grimm, H. In *Antibiotics in Laboratory Medicine*; Lorian, V., Ed.; Williams and Wilkins: Baltimore, MD, 1996; pp 900−1168.

(15) Levy, S. B.; Marshall, B.; Schluederberg, S.; Rowse, D.; Davis, J. High-Frequency of Antimicrobial Resistance in Human Fecal Flora. *Antimicrob. Agents Chemother.* **1988**, *32*, 1801−1806.

(16) Levy, S. B.; Marshall, B. Antibacterial resistance worldwide: causes, challenges and responses. *Nature Med. (N. Y.)* **2004**, *10*, S122−S129.

(17) Zhanel, G. G.; Karlowsky, J. A.; Saunders, M. H.; Davidson, R. J.; Hoban, D. J.; Hancock, R. E. W.; McLean, I.; Nicolle, L. E. Development of Multiple-Antibiotic-Resistant (Mar) Mutants of Pseudomonas-Aeruginosa after Serial Exposure to Fluoroquinolones. *Antimicrob. Agents Chemother.* **1995**, *39*, 489−495.

(18) Bouma, J. E.; Lenski, R. E. Evolution of a bacteria/plasmid association. *Nature* **1988**, *335*.

(19) Schrag, S. J.; Perrot, V.; Levin, B. R. Adaptation to the fitness costs of antibiotic resistance in *Escherichia coli*. *Proc.: Biol. Sci.* **1997**, *264*, 1287.

(20) Jones, M. E.; Boenink, N. M.; Verhoef, J.; Köhrer, K.; Schmitz, F.-J. Multiple mutations conferring ciprofloxacin resistance in *Staphylococcus aureus* demonstrate long-term stability in an antibiotic-free environment. *J. Antimicrob. Chemother.* **2000**, *45*, 353−356.

(21) Smith-Adam, H. J.; Nichol, K. A.; Hoban, D. J.; Zhanel, G. G. Stability of fluoroquinolone resistance in *Streptococcus pneumoniae* clinical isolates and laboratory-derived mutants. *Antimicrob. Agents Chemother.* **2005**, *49*, 846−848.

(22) Renew, J. E. M.S. Thesis, School of Civil and Environmental Engineering, Georgia Institute of Technology: Atlanta, GA, 2003.

(23) Initial decision on proposed withdrawal of Baytril poultry NADA (http://www.fda.gov/cvm/index/updates/baytrilup.htm). U.S. Food and Drug Administration, Center for Veterinary Medicine: Rockville, MD.

(24) Rebenne, L. M.; Gonzalez, A. C.; Olson, T. M. Aqueous chlorination kinetics and mechanism of substituted dihydroxybenzenes. *Environ. Sci. Technol.* **1996**, *30*, 2235−2242.

(25) Gallard, H.; von Gunten, U. Chlorination of phenols: kinetics and formation of chloroform. *Environ. Sci. Technol.* **2002**, *36*, 884−890.

(26) Qiang, Z.; Adams, C. D. Determination of monochloramine formation rate constants with stopped-flow spectrophotometry. *Environ. Sci. Technol.* **2004**, *38*, 1435−1444.

(27) Dodd, M. C.; Huang, C.-H. Transformation of the antibacterial agent sulfamethoxazole in reactions with chlorine: kinetics, mechanisms, and pathways. *Environ. Sci. Technol.* **2004**, *38*, 5607−5615.

(28) *Standard Methods for the Examination of Water and Wastewater*, 20th ed.; APHA, AWWA, WPCF: Washington, 1998.

(29) Pedersen, E. J.; Urbansky, E. T.; Marinas, B. J.; Margerum, D. W. Formation of cyanogen chloride from the reaction of monochloramine with formaldehyde. *Environ. Sci. Technol.* **1999**, *33*, 4239−4249.

(30) Schwarzenbach, R. P.; Gschwend, P. M.; Imboden, D. M. *Environmental Organic Chemistry*, 2nd ed.; John Wiley & Sons: Hoboken, NJ, 2003.

(31) Rule, K. L.; Ebbett, V. R.; Vikesland, P. J. Formation of chloroform and chlorinated organics by free-chlorine-mediated oxidation of triclosan. *Environ. Sci. Technol.* **2005**, *39*, 3176−3185.

(32) Nash, T. The colorimetric estimation of formaldehyde by means of the Hantzsch reaction. *Biochem. J.* **1953**, *55*, 416−421.

(33) Weil, I.; Morris, J. C. Kinetic studies on the chloramines. I. The rates of formation of monochloramine, *N*-chlormethylamine, and *N*-chlordimethylamine. *J. Am. Chem. Soc.* **1949**, *71*, 1664−1671.

(34) *CRC Handbook of Chemistry and Physics*, 82nd ed.; Lide, D. R., Ed.; CRC Press: Boca Raton, FL, 2001.

(35) Ross, D. L.; Riley, C. M. Physicochemical properties of the fluoroquinolone antimicrobials. II. Acid ionization constants and their relationship to structure. *Int. J. Pharm.* **1992**, *83*, 267−272.

(36) Hernández-Borrell, J.; Montero, M. T. Calculating microspecies concentration of zwitterion amphoteric compounds: ciprofloxacin as example. *J. Chem. Educ.* **1997**, *74*, 1311−1314.

(37) Weber, E. J.; Kenneke, J. F. SPARC (http://www.epa.gov/athens/research/projects/sparc). U.S. EPA, National Exposure Research Laboratory: Athens, GA.

(38) Abia, L.; Armesto, M. C. L.; García, M. V.; Santaballa, J. A. Oxidation of aliphatic amines by aqueous chlorine. *Tetrahedron* **1998**, *54*, 521−530.

(39) Morris, J. C. *Kinetics of Reactions between Aqueous Chlorine and Nitrogen Compounds*; John Wiley & Sons: Rutgers University.

(40) Dennis, W. H., Jr.; Hull, L. A.; Rosenblatt, D. H. Oxidations of amines. IV. Oxidative fragmentation. *J. Org. Chem.* **1967**, *32*, 3783−3787.

(41) Stanbro, W. D.; Lenkevich, M. J. Slowly dechlorinated organic chloramines. *Science* **1982**, *215*, 967−968.

(42) Yiin, B. S.; Walker, D. M.; Margerum, D. W. Nonmetal redox kinetics: general-acid-assisted reactions of chloramine with sulfite and hydrogen sulfite. *Inorg. Chem.* **1987**, *26*, 3435−3441.

(43) Yiin, B. S.; Margerum, D. W. Nonmetal redox kinetics: reactions of sulfite with dichloramines and trichloramine. *Inorg. Chem.* **1990**, *29*, 1942−1948.

(44) Bedner, M.; MacCrehan, W. A.; Helz, G. R. Making chlorine greener: investigation of alternatives to sulfite for dechlorination. *Water Res.* **2004**, *38*, 2505−2514.

(45) Gassman, P. G.; Campbell, G. A. Thermal rearrangement of *N*-chloroanilines. Evidence for the intermediacy of nitrenium ions. *J. Am. Chem. Soc.* **1972**, *94*, 3891−3896.

(46) Paul, D. F.; Haberfield, P. Chlorination of anilines. Bimolecular acid-catalyzed rearrangement of *N*-chloroanilines. *J. Org. Chem.* **1976**, *41*, 1, 3170−3175.

(47) Stanbro, W. D.; Smith, W. D. S. Kinetics and mechanism of the decomposition of *N*-chloroalanine in aqueous solution. *Environ. Sci. Technol.* **1979**, *13*, 446−451.

(48) Hand, V. C.; Snyder, M. P.; Margerum, D. W. Concerted Fragmentation of *N*-Chloro-α-Amino Acid Anions. *J. Am. Chem. Soc.* **1983**, *105*, 4022−4025.

(49) Armesto, X. L.; Canle, M.; Garcia, M. V.; Santaballa, J. A. Aqueous chemistry of N-halo-compounds. *Chem. Soc. Rev.* **1998**, *27*, 453−460.

(50) Farinholt, L. H.; Stuart, A. P.; Twiss, D. The halogenation of salicylic acid. *J. Am. Chem. Soc.* **1940**, *62*, 1237−1241.

(51) Grovenstein, E.; Henderson, U. V. Decarboxylation. 3. The Kinetics and Mechanism of Bromodecarboxylation of 3,5-Dibromo-2-Hydroxybenzoic and 3,5-Dibromo-4-Hydroxybenzoic Acids. *J. Am. Chem. Soc.* **1956**, *78*, 569−578.

(52) Larson, R. A.; Rockwell, A. L. Chloroform and chlorophenol production by decarboxylation of natural acids during aqueous chlorination. *Environ. Sci. Technol.* **1979**, *13*, 325−329.

(53) Boyce, S. D.; Hornig, J. F. Reaction pathways of trihalomethane formation from the halogenation of dihydroxyaromatic model compounds for humic acid. *Environ. Sci. Technol.* **1983**, *17*, 202−211.

(54) Itoh, S. I.; Naito, S.; Unemoto, T. Acetoacetic Acid as a Potential Trihalomethane Precursor in the Biodegradation Intermediates Produced by Sewage Bacteria. *Water Res.* **1985**, *19*, 1305−1309.

(55) de la Cruz, A.; Elguero, J.; Goya, P.; Martinez, A.; Pfleiderer, W. Tautomerism and Acidity in 4-Quinolone-3-Carboxylic Acid-Derivatives. *Tetrahedron* **1992**, *48*, 6135−6150.

(56) Bruice, P. Y. Formation of a Carbinolamine Intermediate in the Tertiary Amine Catalyzed Enolization of Oxaloacetic Acid − an Alternative Mechanism for Enolization. *J. Am. Chem. Soc.* **1983**, *105*, 4982−4996.

(57) Prütz, W. A. Reactions of hypochlorous acid with biological substrates are activated catalytically by tertiary amines. *Arch. Biochem. Biophys.* **1998**, *357*, 265−273.

(58) Ellis, A. J.; Soper, F. G. Studies of *N*-halogeno-compounds. Part VI. The kinetics of chlorination of tertiary amines. *J. Chem. Soc.* **1954**, 1750−1755.

(59) Cowan, N. D.; Ludman, C. J.; Waddington, T. C. The Chlorotrimethylammonium and Bromotrimethylammonium Cations. *J. Chem. Soc., Dalton Trans.* **1980**, 821−824.

(60) Masuda, M.; Suzuki, T.; Friesen, M. D.; Ravanat, J.-L.; Cadet, J.; Pignatelli, B.; Nishino, H.; Ohshima, H. Chlorination of guanosine and other nucleosides by hypochlorous acid and myeloperoxidase of activated human neutrophils. *J. Biol. Chem.* **2001**, *276*, 40486−40496.

(61) Buxton, G. V.; Bydder, M.; Salmon, G. A.; Williams, J. E. The reactivity of chlorine atoms in aqueous solution. Part III. The reactions of Cl-center dot with solutes. *Phys. Chem. Chem. Phys.* **2000**, *2*, 237−245.

(62) Snyder, M. P.; Margerum, D. W. Kinetics of chlorine transfer from chloramine to amines, amino acids, and peptides. *Inorg. Chem.* **1982**, *21*, 2545−2550.

(63) Kumar, K.; Day, R. A.; Margerum, D. W. Atom-Transfer Redox Kinetics: General-Acid-Assisted Oxidation of Iodide by Chloramines and Hypochlorite. *Inorg. Chem.* **1986**, *25*, 4344−4350.

(64) Isaac, R. A.; Morris, J. C. Transfer of active chlorine from chloramine to nitrogenous organic compounds. 2. Mechanism. *Environ. Sci. Technol.* **1985**, *19*, 810−814.

(65) Gray, E. T., Jr.; Margerum, D. W.; Huffman, R. P. In *Organometals and Organometalloids, Occurrence and Fate in the Environment*; Brinkman, F. E., Bellama, J. M., Eds.; American Chemical Society: Washington, DC, 1978; pp 264−277.

(66) Clark, M. M. *Transport Modeling for Environmental Engineers and Scientists*; John Wiley & Sons: New York, 1996.

(67) Shen, L. L.; Mitscher, L. A.; Sharma, P. N.; O'Donnell, T. J.; Chu, D. W. T.; Cooper, C. S.; Rosen, T.; Pernet, A. G. Mechanism of inhibition of DNA gyrase by quinolone antibacterials: a cooperative drug−DNA binding model. *Biochemistry* **1989**, *28*, 3886−3894.

(68) Vázquez, J. L.; Berlanga, M.; Merino, S.; Domènech, Ò.; Viñas, M.; Montero, M. T.; Hernández-Borrell, J. Determination by fluorimetric titration of the ionization constants of ciprofloxacin in solution and in the presence of liposomes. *Photochem. Photobiol.* **2001**, *73*, 14−19.

(69) Barbosa, J.; Barrón, D.; Jiménez-Lozano, E.; Sanz-Nebot, V. Comparison between capillary electrophoresis, liquid chromatography, potentiometric, and spectrophotometric techniques for evaluation of pK_a values of zwitterionic drugs in acetonitrile-water mixtures. *Anal. Chim. Acta* **2001**, *437*, 309−321.

(70) Barbosa, J.; Barrón, D.; Cano, J.; Jiménez-Lozano, E.; Sanz-Nebot, V.; Toro, I. Evaluation of electrophoretic method versus chromatographic, potentiometric, and absorptiometric methodologies for determining pK_a values of quinolones in hydro-organic mixtures. *J. Pharm. Biomed. Anal.* **2001**, *24*, 1087−1098.